THE JOURNAL OF BIOLOGICAL CHEMISTRY VOL. 288, NO. 28, pp. 20758–20767, July 12, 2013

Two Salt Bridges Differentially Contribute to the Maintenance of Cystic Fibrosis Transmembrane Conductance Regulator (CFTR) Channel Function*[S]

Received for publication, April 9, 2013, and in revised form, May 20, 2013 Published, JBC Papers in Press, May 24, 2013, DOI 10.1074/jbc.M113.476226

Guiying Cui, Cody S. Freeman, Taylor Knotts, Chengyu Z. Prince, Christopher Kuang, and Nael A. McCarty[1]

From the Division of Pulmonology, Allergy/Immunology, Cystic Fibrosis, and Sleep, Department of Pediatrics, Center for Cystic Fibrosis Research, Emory University School of Medicine and Children's Healthcare of Atlanta, Atlanta, Georgia 30322

Background: Two salt bridges, Arg^{347}–Asp^{924} and Arg^{352}–Asp^{993}, have been identified in CFTR, but the timing of their interaction remains unknown.
Results: Arg^{347}-Asp^{924}-Asp^{993} form a triangular salt bridge and work together with the Arg^{352}-Asp^{993} salt bridge to maintain the open pore architecture of CFTR.
Conclusion: These salt bridge residues interact and contribute differently in stabilizing the open pore during gating cycle.
Significance: Understanding the CFTR pore dynamic open-closed transition is crucial for rational drug design.

Previous studies have identified two salt bridges in human CFTR chloride ion channels, Arg^{352}-Asp^{993} and Arg^{347}-Asp^{924}, that are required for normal channel function. In the present study, we determined how the two salt bridges cooperate to maintain the open pore architecture of CFTR. Our data suggest that Arg^{347} not only interacts with Asp^{924} but also interacts with Asp^{993}. The tripartite interaction Arg^{347}-Asp^{924}-Asp^{993} mainly contributes to maintaining a stable s2 open subconductance state. The Arg^{352}-Asp^{993} salt bridge, in contrast, is involved in stabilizing both the s2 and full (f) open conductance states, with the main contribution being to the f state. The s1 subconductance state does not require either salt bridge. In confirmation of the role of Arg^{352} and Asp^{993}, channels bearing cysteines at these sites could be latched into a full open state using the bifunctional cross-linker 1,2-ethanediyl bismethanethiosulfonate, but only when applied in the open state. Channels remained latched open even after washout of ATP. The results suggest that these interacting residues contribute differently to stabilizing the open pore in different phases of the gating cycle.

Cystic fibrosis transmembrane conductance regulator (CFTR),[2] a 1480-amino acid transmembrane protein, is the only member of the ATP-binding cassette (ABC) transporter superfamily that is known to behave as a Cl^- ion channel. Dysfunction of CFTR is directly associated with three devastating diseases: cystic fibrosis, polycystic kidney disease, and secretory diarrhea. Based on functional data and homology models, CFTR has been predicted to contain five functional domains: two membrane-spanning domains (MSDs), each including six transmembrane (TM) helices; two nucleotide binding domains (NBD1 and NBD2); and a unique regulatory (R) domain, which carries multiple protein kinase A (PKA) consensus phosphorylation sites and is unique to CFTR in the ABC superfamily (1–6). Functional studies from multiple groups have suggested that TM6 plays an essential role and TM12 contributes less to anion conduction and permeation properties in the CFTR channel pore (7–11).

CFTR channel pore opening is accomplished by R domain phosphorylation and the binding of ATP at the NBDs, where the two MSDs are driven to change conformation to allow anions to flow. It remains unclear how the CFTR channel pore moves during the gating cycle, including whether it passes through multiple conductance states or simply switches directly between fully "closed" (c) and fully "open" (f) states. We reported previously that human wild type CFTR (WT-CFTR) exhibits a predominant full open state with two rare subconductance states (s1 and s2). Infrequent subconductance behavior is seen in some CFTR mutants, such as T338A/C- and S1141A-CFTR (7, 12). However, subconductance states are dominant events with short burst durations in CFTR channels bearing known salt bridge mutations, such as R352A, R347H, D993R, and D924R (13, 14). When arginine 334 at the extracellular end of TM6 is mutated to A or C, both mutants show s1 and s2 as the dominant open states with only brief transitions to the f state (15). Mutation D1152A in the inner vestibule of TM12 results in channels that frequently exhibit the s1 and s2 open states as well as the f open state (7). In the mutant channels exhibiting prominent subconductance states, the sequence of occupancy of the s1, s2, and f states does not appear to be random (12, 16). For example, R334C-CFTR channels routinely open to the s1 and then s2 states and transition to the f state just before closing (15). Hence, it is reasonable to believe that CFTR channel pore opening might involve a complicated sequence of multiple steps leading to the occupancy of a stable, full open state.

* This work was supported, in whole or in part, by National Institutes of Health Grant R01-DK056481 (to N. M.).
[S] This article contains supplemental Figs. 1–5.
[1] To whom correspondence should be addressed: Division of Pulmonology, Allergy/Immunology, Cystic Fibrosis, and Sleep, Department of Pediatrics, Center for Cystic Fibrosis Research, Emory University School of Medicine and Children's Healthcare of Atlanta, 2015 Uppergate Dr., Atlanta, GA 30322. Tel.: 404-727-3654; Fax: 404-712-0920; E-mail: namccar@emory.edu.
[2] The abbreviations used are: CFTR, cystic fibrosis transmembrane conductance regulator; TES, 2-{[2-hydroxy-1,1-bis(hydroxymethyl)ethyl]amino} ethanesulfonic acid; NP_o, open probability times number of channels; ABC, ATP-binding cassette transporter; MSD, membrane-spanning domain; TM, transmembrane; NBD, nucleotide binding domain; MTS, methanethiosulfonate; MTS-2-MTS, 1,2-ethanediyl bismethanethiosulfonate.

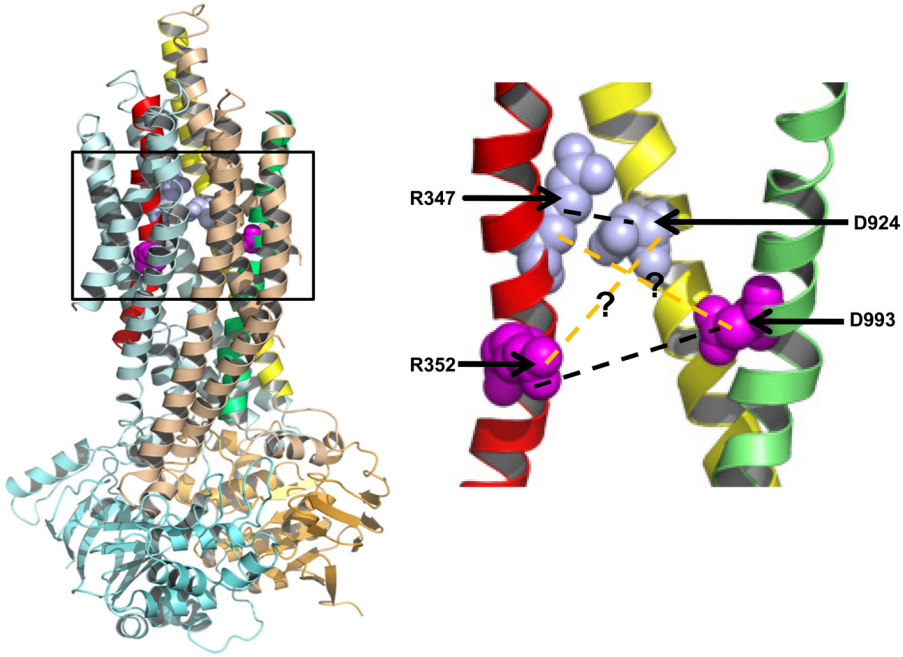

FIGURE 1. **CFTR homology model indicating two salt bridges, using the homology model from the Riordan group (5).** *Left*, the whole CFTR homology model with *frame* indicating the segment shown enlarged at the *right*. *Right*, *close-up view* of the residue pairs Arg^{347}-Asp^{924} and Arg^{352}-Asp^{993}. *Pale cyan*, TMD1; *light brown*, TMD2; *cyan*, NBD1; *light orange*, NBD2. The TM domains involved in these salt bridges are *colored* as follows: TM6 (*red*), TM8 (*yellow*), and TM9 (*green*). The previously described Arg^{352} (TM6)-Asp^{993} (TM9) salt bridge and the Arg^{347} (TM6)-Asp^{924} (TM8) salt bridge in CFTR are shown *connected* with *dark dashed lines*. The predicted interaction between Arg^{347} and Asp^{993} is depicted with *orange dashed lines*.

Two pore domain salt bridges, Arg^{347}-Asp^{924} and Arg^{352}-Asp^{993}, have been identified that contribute to maintaining the open pore architecture of CFTR (13, 14). Fig. 1 shows the CFTR homology model from the Riordan group with all four salt bridge amino acids labeled (5). The channel state of CFTR in the homology model is unclear, but it is evident that the four salt bridge amino acids sit close to each other. Alexander *et al.* found that Arg^{352} and Asp^{993} start out quite a distance away from each other in their molecular dynamics simulations of CFTR conformational change and move toward to each other as the simulation progresses toward the open state (3). In the bacterial Na^+ channel and Kv7.1 channels, it has been reported that dynamic electrostatic interactions are involved in channel gating (17–20). Regarding the two salt bridges identified in CFTR, Arg^{347}-Asp^{924} and Arg^{352}-Asp^{993}, questions remaining include the following. 1) How do the two salt bridges cooperate to maintain the CFTR channel pore in the correct architecture for normal channel behavior? 2) Do the salt bridges form coincidentally or sequentially? 3) Do they contribute to the s1, s2, and f conduction states equally or divergently?

Disulfide bond formation between substituted cysteine residues has proven to be a powerful tool to analyze the structure and function of channel proteins (17–19). Here we have adapted these methods combined with site-directed mutagenesis and single channel recording techniques to analyze the interactions and cooperation between these four charged residues: Arg^{347}, Asp^{924}, Arg^{352}, and Asp^{993}. Our results demonstrate that Arg^{347}, Asp^{924}, and Asp^{993} form a triangular salt bridge early in channel openings, whereas Arg^{352} and Asp^{993} interact late in channel opening. These results contribute to our understanding of how CFTR gained ion channel function despite its origin in the ABC transporter superfamily.

EXPERIMENTAL PROCEDURES

Preparation of Oocytes and cRNA—The mutants used in this study were prepared using site-directed mutagenesis with the QuikChange protocol (Stratagene, La Jolla, CA). All cRNAs for single channel recording were prepared from constructs encoding WT-CFTR or Cys-less CFTR (16C → S, C590L, C592L) in the pGEMHE vector, which was kindly provided by Dr. D. Gadsby (Rockefeller University) as reported previously (21). *Xenopus laevis* oocytes were injected in a range of 1–10 ng of CFTR cRNAs and were incubated at 18 °C in modified L-15 medium (12). Methods of animal handling were in accordance with National Institutes of Health guidelines, and the protocol was approved by the Institutional Animal Care and Use Committee of Emory University.

Electrophysiology—For single channel recording, CFTR channels were studied in excised, inside-out patches at room temperature (22–23 °C). Oocytes were prepared for study by shrinking in hypertonic solution, followed by manual removal of the vitelline membrane (12). Pipettes were pulled from borosilicate glass (Sutter Instrument Co., Novato, CA) and had resistances averaging ~10 megaohms when filled with chloride-containing pipette solution (150 mM NMDG-Cl, 5 mM $MgCl_2$, 10 mM TES (pH 7.5)). Typical seal resistances were 200 gigaohms or greater. Channels were activated by excision into intracellular solution containing 150 mM NMDG-Cl, 1.1 mM $MgCl_2$, 2 mM Tris-EGTA, 10 mM TES, 1 mM MgATP, and 50 units/ml PKA (pH 7.5). CFTR currents were measured with an Axopatch 200B amplifier (Molecular Devices, Sunnyvale, CA) and were recorded at 10 kHz to DAT tape. For subsequent analysis, records were played back and filtered with a four-pole Bessel filter (Warner Instruments, Hamden, CT) at a corner

frequency of 1 kHz and acquired using a Digidata 1322A interface and computer at 500 Hz with pClamp 8.2. For display, single channel records were filtered digitally to 100 Hz.

Open burst duration analysis was performed on records from patches containing 1–3 active CFTR channels using Clampfit version 9.0. Figures were made in Sigmaplot version 8.0. The mean open duration in multichannel patches was determined as described previously (15). Then we measured the fraction of open burst duration for s1, s2, and f, as follows.

$$\text{Fraction of burst duration for s1} = s1/(s1 + s2 + f) \quad \text{(Eq. 1)}$$

$$\text{Fraction of burst duration for s2} = s2/(s1 + s2 + f) \quad \text{(Eq. 2)}$$

$$\text{Fraction of burst duration for f} = f/(s1 + s2 + f) \quad \text{(Eq. 3)}$$

Energetic Mutant Cycle Analysis—We adapted this technique from the recent publications from the Sine group (22). Open burst durations and closed durations were measured from single channel recordings of WT-, R352C-, D993C-, and R352C/D993C-CFTR, and then histograms and fits of them with single exponential functions were generated with IGOR (WaveMetrics, Inc., Lake Oswego, OR) to determine time constants for open burst durations (τ_o, also called β) and closed durations (τ_c, also called α) for all of the constructs. The gating equilibrium constant θ was calculated using Equation 4.

$$\theta = \beta/\alpha \quad \text{(Eq. 4)}$$

The free energy change for each mutant relative to WT-CFTR was calculated as follows.

$$\Delta G = -RT \ln(\theta_{mutant}/\theta_{WT}) \quad \text{(Eq. 5)}$$

Then total energy change between WT and the double mutant was calculated using Equation 6,

$$\Delta\Delta G = -RT \ln(\theta_{ww}\theta_{mm}/\theta_{wm}\theta_{mw}) \quad \text{(Eq. 6)}$$

where ww represents wild type, mm is double mutant, wm and mw are single mutants, R is the universal gas constant (1.987 cal/K/mol), and T is the absolute temperature (293 K).

Source of Reagents and Antibodies—Unless otherwise noted, all reagents were obtained from Sigma. L-15 medium was from Invitrogen. All MTS reagents were from Toronto Research Chemicals Inc. (Ottawa, Canada). PKA was from Promega (Madison, WI). MTS reagents were prepared as a stock solution at 0.1 M in DMSO or H_2O and diluted to 100 μM immediately before use.

Statistics—Unless noted, values given are mean ± S.E. Statistical analysis was performed using Student's t test for unpaired or paired measurements by Sigma Stat version 2.03 (Jandel Scientific, San Rafael, CA), with $p < 0.05$ considered indicative of significance.

RESULTS

Arg^{347} Forms a Salt Bridge with Asp^{924} but Does Not Stabilize the Full Open State—Although Cotten and Welsh first reported that arginine 347 of TM6 forms a salt bridge with aspartic acid 924 of TM8, their results suggested that the double mutation R347D/D924R rescued the channel to a stable open state that exhibits a smaller single channel amplitude, which is reminiscent of the s2 open state of WT-CFTR (14). We asked whether the Arg^{347}-Asp^{924} salt bridge can completely rescue the CFTR channel to a full WT-CFTR open state. We generated single and double mutants at Arg^{347} and Asp^{924} and studied their behavior in excised, inside-out single channel patches pulled from *Xenopus* oocytes expressing these CFTR proteins. Representative data from these mutants are shown in Fig. 2*A*, whereas summaries of the fraction of each open burst represented by s1, s2, and f states are provided in Fig. 2*B*. The main features of each mutant channel, with respect to open state behavior, are summarized in Table 1.

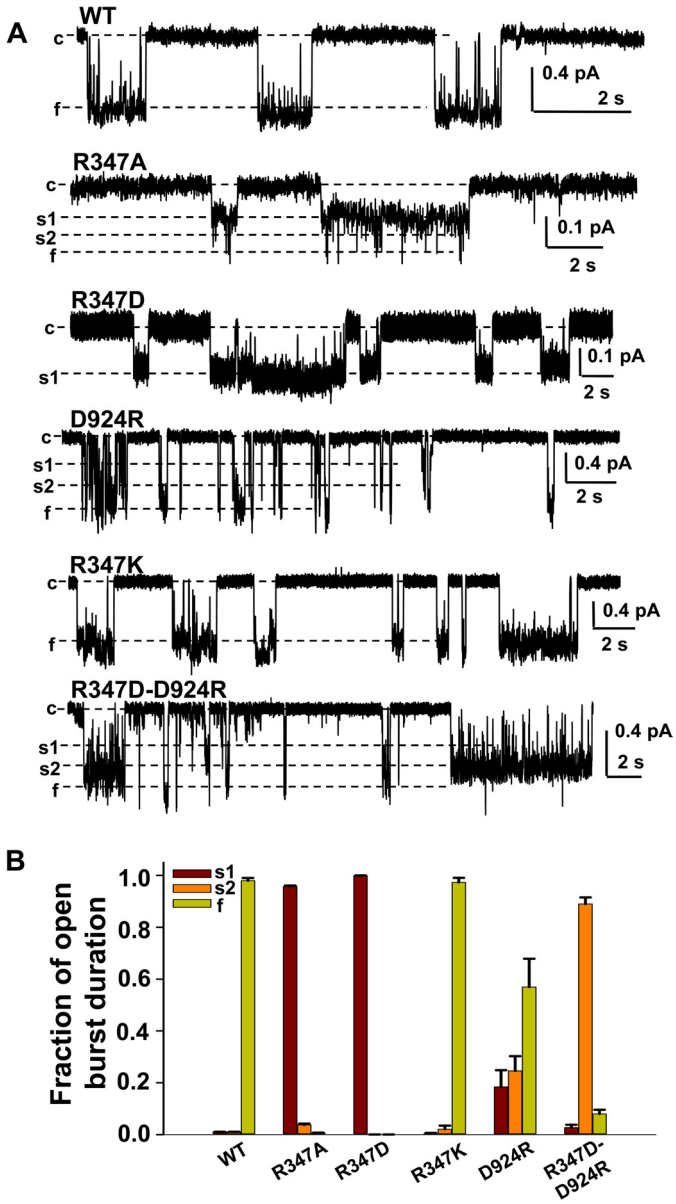

FIGURE 2. **Arg^{347} forms a salt bridge with Asp^{924}.** *A*, representative current samples of WT-, R347A-, R347D-, D924R-, R347K-, and R347D/D924R-CFTR were recorded from excised inside-out patch from *Xenopus* oocytes with 150 mM Cl^- symmetrical solution in the presence of 1 mM Mg-ATP and 50 nM PKA at $V_M = -100$ mV ($n = 4–6$ for each mutant). *c*, closed state; *s1*, subconductance state 1; *s2*, subconductance state 2; *f*, full open state. *B*, mean fraction of open burst duration is plotted for each state of the six CFTR mutants. For each of the open conductance states, s1 is shown in *purple*, s2 in *orange*, and f in *light green*. *Error bars*, S.E.

TABLE 1
Summary of the effects of mutations studied

Mutant	Main features of open bursts	Impact on f state
R347A	Emphasizes s1 state, brief transitions to s2 and f	Can reach f but not stable
R347D	Emphasizes s1 state, no transitions to s2 and f	Cannot reach f
D924R	Brief transitions to all conductance levels	Can reach f but not stable
R347K	Wild type-like	Wild type-like
R347D/D924R	Emphasizes s2 state, rare and brief transitions to f	Can reach f but not stable
R352E	Opens to all 3 levels; s1 much more stable than in WT, s2 unstable, f unstable	Can reach f but not stable
D993R	Opens to all 3 levels, but none are stable	Can reach f but not stable
R352E/D993R	Wild type-like, with increased transitions to s1 and s2; slightly reduced single-channel conductance	Wild type-like
R352E/D924R	Opens to all 3 levels, but none are stable	Can reach f but not stable
R347D/D993R	Very stable s2; rare and brief transitions to both s1 and f	Can reach f but not stable
R347A/R352A	Opens to all 3 levels; s1 much more stable than in WT, s2 unstable, f unstable	Can reach f but not stable
R347D/D924R/D993R	Opens to all 3 levels; s1 much more stable than in WT, s2 relatively stabilized, f unstable	Can reach f but not stable
R347D/D924R/R352E/D993R	Primarily flickers between s2 and f; s1 much more stable than in WT, slightly reduced single channel conductance	Can reach f but not stable

The WT-CFTR single channel trace in Fig. 2*A* exhibits stable sojourns in the open (f) and closed (c) states with s1 and s2 represented as brief events. R347A-CFTR showed a very long and stable s1 state with very brief openings to s2 or f states, whereas R347D-CFTR only exhibits a long stable s1 state and appears to never get out of s1 (at the resolution of our recording apparatus), as if introduction of negative charge at this position confers electrostatic repulsion with other negative charges in the native channel and thereby greatly interferes with the ability to go beyond the s1 state. R347K-CFTR, retaining the positive charge of arginine, showed behavior similar to WT-CFTR (-0.72 ± 0.02 pA, $n = 7$) but with a slightly larger single channel amplitude (-0.89 ± 0.01 pA, $n = 4, p < 0.05$). D924R-CFTR exhibits all three open states in contrast to R347A- and R347D-CFTR, although the stability of the open state is compromised; indeed, the fractional occupancies of both s1 and s2 states are greatly increased in this mutant (Fig. 2*B*). The charge-swapping double mutant R347D/D924R-CFTR exhibited a long stable s2 state with occasional brief openings to s1 and f. The most stable open state exhibited single channel amplitude (-0.52 ± 0.01 pA, $n = 5$) equivalent to ~70% of WT-CFTR, consistent with our previous designation of the s2 open state (12, 16). In all of the Arg^{347} and Asp^{924} mutants described above, other than R347K, transitions to the f state did not lead to stable occupancy of that state. These results suggest that strengthening the Arg^{347}-Asp^{924} salt bridge is not able to completely rescue CFTR to the full open state but at best can stabilize the s2 state. In addition, breaking this salt bridge disrupted the stability of the s2 and f states but did not significantly affect s1; therefore, both R347A and R347D showed long stable s1 states, although R347A endeavored to reach the s2 and f states but failed to maintain them, whereas R347D completely lost the ability to open to s2 and f state.

These data suggest that the Arg^{347}-Asp^{924} salt bridge contributes strongly to the stability of the s2 state but at best makes only a weak contribution to the stability of the f state. In contrast, we have shown that interaction between Arg^{352} and Asp^{993} is required for stabilizing the open state (13). In our prior studies, we found that R352E-CFTR can open to all three conductance levels, with all open states being unstable. Similar results were found for D993R-CFTR, but nearly wild type-like behavior, including stable openings to the f state, was recovered in the R352E/D993R double mutant (see Fig. 3*A*). This comparison of behavior in the double mutants supports the notion that

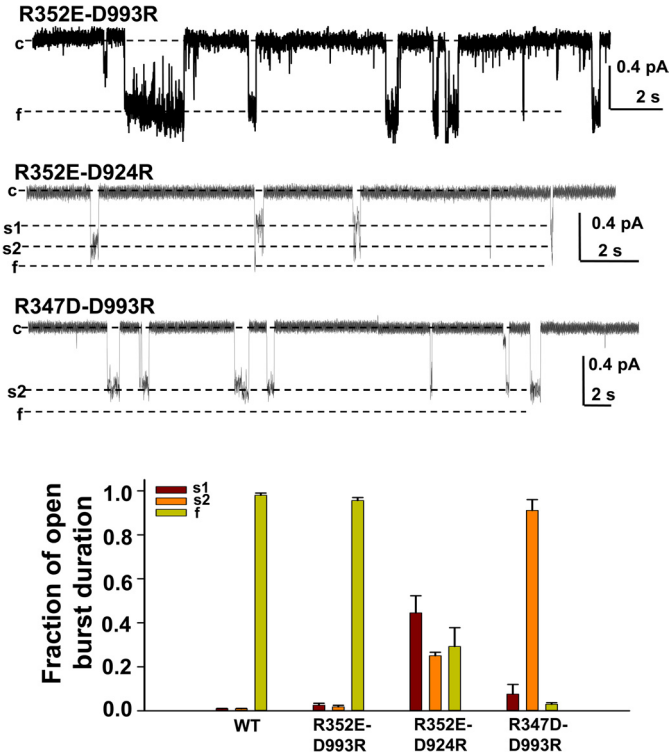

FIGURE 3. **Asp^{993} is a salt bridge partner of Arg^{352} as well as of Arg^{347}.** *A*, representative current samples of R352E/D993R-, R352E/D924R-, and R347D/D993R-CFTR recorded from excised inside-out patches with the same conditions as Fig. 2 ($n = 3$–6 for each mutant). *B*, mean fraction of open burst duration is plotted for each state of three CFTR mutants, for each of the open conductance states: s1 (*purple*), s2 (*orange*), and f (*light green*). *Error bars*, S.E.

the Arg^{347}-Asp^{924} and Arg^{335}-Asp^{993} salt bridges make different contributions to the stability of open CFTR channels.

Asp^{993} Interacts with Arg^{352} as Well as Arg^{347}—The above results suggest that the Arg^{347}-Asp^{924} salt bridge is unable to fully rescue CFTR channel pore stability; consequently, it is possible that Arg^{347} might interact with another negative charge to form a triangular salt bridge, as occurs in cyclic nucleotide-gated channels and hyperpolarization-activated cyclic nucleotide-modulated channels (23, 24). Exploration of the four published CFTR homology models and our former work suggested that Arg^{347} also approaches Asp^{993} in the open state (1–3, 5, 14). We therefore hypothesized that Arg^{347} might also interact with Asp^{993} to rescue the CFTR channel pore to a stable f state and tested this hypothesis in three double mutants;

representative data are shown in Fig. 3 and summarized in Table 1. As noted above, R352E/D993R exhibited a prominent full open state similar to WT-CFTR (13), suggesting that the R352E/D993R salt bridge can fully rescue the CFTR channel pore to normal behavior (aside from a slight decrease in single channel conductance). Whereas the single channel behavior of R352E/D924R was similar to that of R352E alone, with multiple unstable open states, suggesting that Arg^{352} and Asp^{924} do not interact, R347D/D993R was much more like R347D/D924R, with the s2 state dominant (compare Figs. 3 and 2). R347D/D993R-CFTR is able to transition to the f state but sojourns there are even more brief than those seen for the R347D/D924R. These data strongly indicate that Arg^{347} interacts with both Asp^{924} and Asp^{993} to maintain the CFTR channel pore open architecture. This is in partial agreement with the findings of Cotten and Welsh (14), who only showed Arg^{347} interacting with Asp^{924}. In contrast, Arg^{352} only interacts with Asp^{993}, as we have reported previously (13).

Two Salt Bridges Work Together to Maintain Normal Architecture of the CFTR Channel Pore—The data so far show that Arg^{347} can interact with both Asp^{924} and Asp^{993}. In the R347D/D924R mutant, the positive charge at Arg^{347} is no longer available to interact with Asp^{993}. Similarly, in the R347D/D993R mutant, the positive charge at Arg^{347} is no longer available to interact with Asp^{924}. Therefore, we asked whether replacing the negative charge at both Asp^{924} and Asp^{993} with a positive charge would allow strong enough interactions with R347D to enable channels to go to the f state. This was tested in the triple mutant R347D/D924R/D993R (Fig. 4, *A* and *B*). Unlike the two double mutants described above (R347D/D924R and R347D/D993R), the triple mutant exhibited roughly equal occupancy of s1, s2, and f states; the occupancy of the s2 state was not as stable as in either double mutant. The triple mutant exhibited little stability of either state, suggesting that WT-like stability of the f state requires more than the sum of these two-way interactions.

Both Arg^{347} and Arg^{352} contribute to intraprotein interactions important to CFTR channel gating, and we have shown that interaction between Arg^{352} and Asp^{993} is required for stabilizing the f state, whereas interactions between Arg^{347} and both Asp^{924} and Asp^{993} are required for stabilizing the s2 state. We then asked how these three interactions work together to stabilize CFTR channel behavior. As we show in Fig. 4, R347A/R352A-CFTR behaves just like R352A-CFTR, opening to all three conductance states with little stability of either state, as we reported before. These results indicate that CFTR channels are able to reach each of the conductance levels in the absence of both salt bridges, but they are unable to stabilize the occupancy of either open conductance level. In R352A-CFTR, Arg^{347} can still interact with Asp^{924} and Asp^{993}. However, those interactions are not strong enough to overcome the instability arising from the loss of positive charge at Arg^{352} (13). These data suggest that interactions at Arg^{352} are dominant over the interactions at Arg^{347}.

In summary, from the data that we have presented so far, we conclude that CFTR channels can reach all of the conductance levels even without either of these salt bridge interactions. Neither salt bridge is active in the s1 state, suggesting that s1 is a base-line open state conformation resulting from the dimerization of the NBDs before either of the salt bridges form their interactions. State s2 is primarily maintained by the triangular salt bridge in which Arg^{347} interacts with both Asp^{924} and Asp^{993}. The f open state mainly depends on the Arg^{352}-Asp^{993} salt bridge. Arg^{347} probably still interacts with Asp^{924} in the f state, but that interaction is not strong enough to maintain stability of the f state in the absence of the Arg^{352}-Asp^{993} salt bridge. Furthermore, because Asp^{993} is shared by two salt bridges, it is reasonable to believe that Asp^{993} might switch between its two salt bridge partners, interacting with Arg^{347} or Arg^{352} in a sequential rather than coincidental manner.

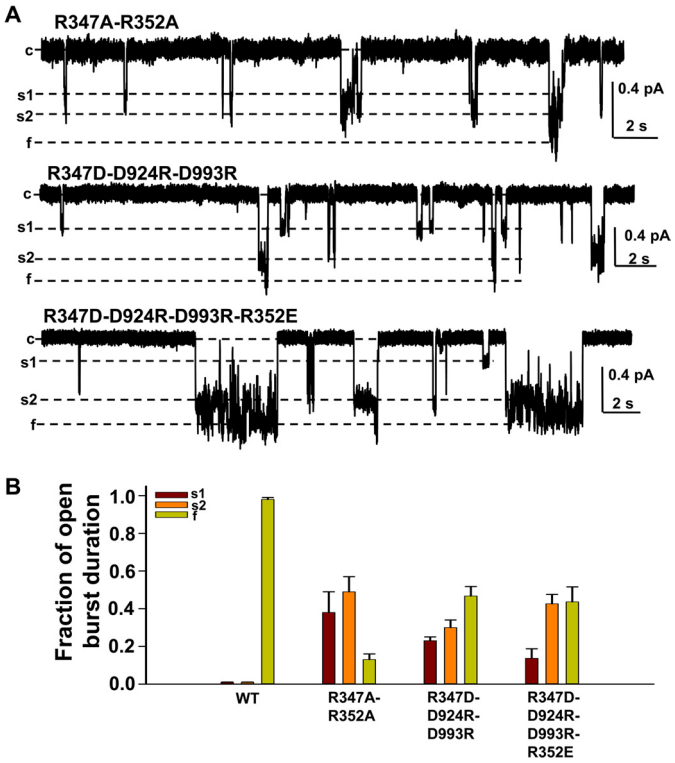

FIGURE 4. **The triangular salt bridge Arg^{347}-Asp^{924}-Asp^{993} and salt bridge Arg^{352}-Asp^{993} cooperate together to stabilize the CFTR open pore in a normal architecture.** Representative current samples of R347A/R352A-, R347D/D924R/D993R-, and R347D/D924R/D993R/R352E-CFTR were recorded under the same conditions as in Fig. 3 ($n = 5–6$ for each mutant) (*A*). The mean fraction of open burst duration for each state of three CFTR mutants is shown in *B*. For all mutants, s1 is shown in *dark red*, s2 in *orange*, and f in *light green*. *Error bars*, S.E.

Because the above results suggested that two salt bridges play roles in stabilizing the open states of CFTR, we asked whether a quadruple mutant, bearing charge swaps at each of the four residues involved in these two salt bridges, might behave similarly to WT-CFTR channels. However, the quadruple mutant R347D/D924R/D993R/R352E did not completely rescue WT behavior (Fig. 4, *A* and *B*). These channels were able to occupy all three open states but were most stable in the s2 and f states, with occupancy in s1 slightly more stable than in WT-CFTR (<20%). As shown in the trace in Fig. 4*A*, quadruple mutant channels exhibited frequent and brief transitions between the s2 and f states, suggesting that the channels can easily achieve the s2 state and can reach the f state, but the interactions are not strong enough to maintain the f state conformation. These incomplete responses to charge swap may arise from small dif-

ferences in side-chain orientation in the quadruple mutant compared with in the WT channels, which could alter both the strength and the timing of electrostatic interactions.

MTS Reagents Exhibit No Effects on Single Channel Amplitude of WT-CFTR and Cys-less V510A-CFTR—Because the Arg^{352}-Asp^{993} interaction appeared to make the largest contribution to stabilizing the f state, we asked whether forcing these residues to interact would lead to channels that were latched into the open state. We took advantage of the ability to cross-link cysteines engineered into known positions using bifunctional sulfhydryl-modifying reagents of known length. We generated R352C/D993C-CFTR and exposed the channels to MTS-2-MTS; MTS-2-MTS was chosen for this experiment because it leads to cross-linking of cysteines at a distance of ~4.6 Å, which is within the average distance for known salt bridges in a variety of proteins (13). Prior to studies with the double mutant, we also investigated each single mutant and their responses to monofunctional sulfhydryl-modifying reagents.

As controls for these experiments, we first asked whether WT channels were sensitive to modification by monofunctional or bifunctional sulfhydryl-modifying reagents. Because 14 of 18 endogenous cysteines in WT-CFTR are predicted to be localized to the intracellular side of the protein, making them possible targets of MTS-induced modification, we also made use of the Cys-less CFTR construct (kind gift of D. Gadsby). We further added a secondary mutation to generate Cys-less V510A-CFTR in order to improve expression (9, 25). Because it was reported that Cys-less CFTR showed channel behavior similar to that of WT-CFTR with a few nominal differences (9, 26–28), we first used mutants generated on the WT-CFTR background and then confirmed the results in mutants generated on the Cys-less V510A-CFTR background. Representative data indicating that charged monofunctional MTS reagents modified the activity of WT-CFTR or Cys-less V510A-CFTR when applied cytoplasmically in excised, inside-out patches are shown in supplemental Fig. 1. Supplemental Fig. 1*A* shows results for WT-CFTR in the absence and presence of $MTSET^+$, which did not change single channel amplitude (~0.73 pA) or mean burst duration (684 ms before $MTSET^+$ and 693 ms after $MTSET^+$); similar phenomena were seen for WT-CFTR in the presence of $MTSEA^+$ and $MTSES^-$. Unlike the lack of effects on ion conduction, positively charged $MTSET^+$ and $MTSEA^+$ affected WT-CFTR channel gating by increasing NP_o, whereas negatively charged $MTSES^-$ decreased NP_o, probably by modifying cysteines located in the cytoplasmic domains of CFTR (supplemental Fig. 1); modification was covalent because the effects were not typically terminated by washout and yet were reversed by exposure to 1 mM DTT. Supplemental Fig. 1*B* shows Cys-less V510A-CFTR in the absence and presence of MTS reagents; not surprisingly, MTS reagents exhibited no effects on either single channel amplitude or NP_o in the Cys-less channel. Based on these results, we resolved to use both WT-CFTR and Cys-less V510A-CFTR as backgrounds to test the consequences of modification of engineered cysteines.

Recovery of Charge at R352C and D993C Rescued Channel Stability in the Full Open State—R352C-CFTR exhibited single channel behavior similar to that previously reported for R352A-, R352Q-, and R352E-CFTR (13). A representative recording is shown in Fig. 5*A*, taken from one membrane patch bearing R352C-CFTR before and after exposure to $MTSEA^+$ and after wash out. A segment of each current trace recorded under the three conditions is shown in expanded resolution. Prior to exposure to $MTSEA^+$, R352C-CFTR exhibited multiple conductance states, including closed (c) and s1, s2, and f open states. R352C-CFTR channels opened to all open states for very short durations (Fig. 5*B*). After exposure to $MTSEA^+$, R352C-CFTR channels exhibited mainly the f state with much longer mean burst duration and appearance of the s1 and s2 states as rare events, indicating recovery of open state stability (Fig. 5*B*). Channels closed upon washout of ATP, PKA, and $MTSEA^+$. Exposure to $MTSEA^+$ did not affect the absolute amplitude of the s1 and s2 states but significantly decreased the conductance of the f state (Fig. 5*C*), which may arise from the partial blockade of ion conduction in the CFTR pore by the bulky MTS reagent ($n = 5$); the latter result is inconsistent with Arg^{352} contributing to a chloride binding site, as suggested previously (29). Similar results were found when the channels were exposed to $MTSET^+$. In contrast, deposition of negative charge at R352C-CFTR by exposure to $MTSES^-$ did not alter channel behavior (supplemental Fig. 2*A*). As a control, we show that R352A-CFTR was not sensitive to modification by MTS reagents (supplemental Fig. 2*B*). These data suggest that covalent deposition of positive charge at position 352 with $MTSET^+$ or $MTSEA^+$ rescued the intraprotein interaction represented in the wild type channel by the Arg^{352}-Asp^{993} salt bridge. We note that in R352C-CFTR on the WT-CFTR background, exposure to $MTSEA^+$ and $MTSET^+$ led to an increase in NP_o (Fig. 5*A*), reflecting modification of endogenous cysteines. This added effect was lost on the Cys-less V510A background. In contrast to these results for R352C-CFTR, the stability of single channel opening in D993C-CFTR was rescued to mimic that of WT-CFTR by exposure to $MTSES^-$ (but not $MTSEA^+$ or $MTSET^+$), leading to significantly increased mean burst duration (supplemental Fig. 3*B*). Exposure to $MTSES^-$ also significantly decreased the conductance of the f state of D993C-CFTR (supplemental Fig. 3*B*).

Taken together, these results support the existence of a charge-charge interaction between Arg^{352} and Asp^{993} and also suggest that these residues face the aqueous pore during at least part of the gating cycle because both cysteines were accessible to modification by MTS reagents. We repeated the above experiments in R352C/Cys-less V510A-CFTR and D993C/Cys-less V510A-CFTR to further rule out the possibility of any endogenous cysteines being involved in the process. Representative experiments are shown in supplemental Fig. 4. These effects were removed only upon application of the reducing agent DTT and indicate that the Cys-less V510A-CFTR background was identical to the WT-CFTR background with respect to these experiments.

A Bifunctional MTS Reagent Can Latch R352C/D993C-CFTR into the Full Open State Even after Washout of ATP—We hypothesized that the CFTR channel pore could be latched into the open state by cross-linking the two cysteines at R352C and D993C. We first tested the effects of monofunctional reagents $MTSET^+$, $MTSEA^+$, and $MTSES^-$ on the double mutant R352C/D993C-CFTR. None of these reagents rescued salt

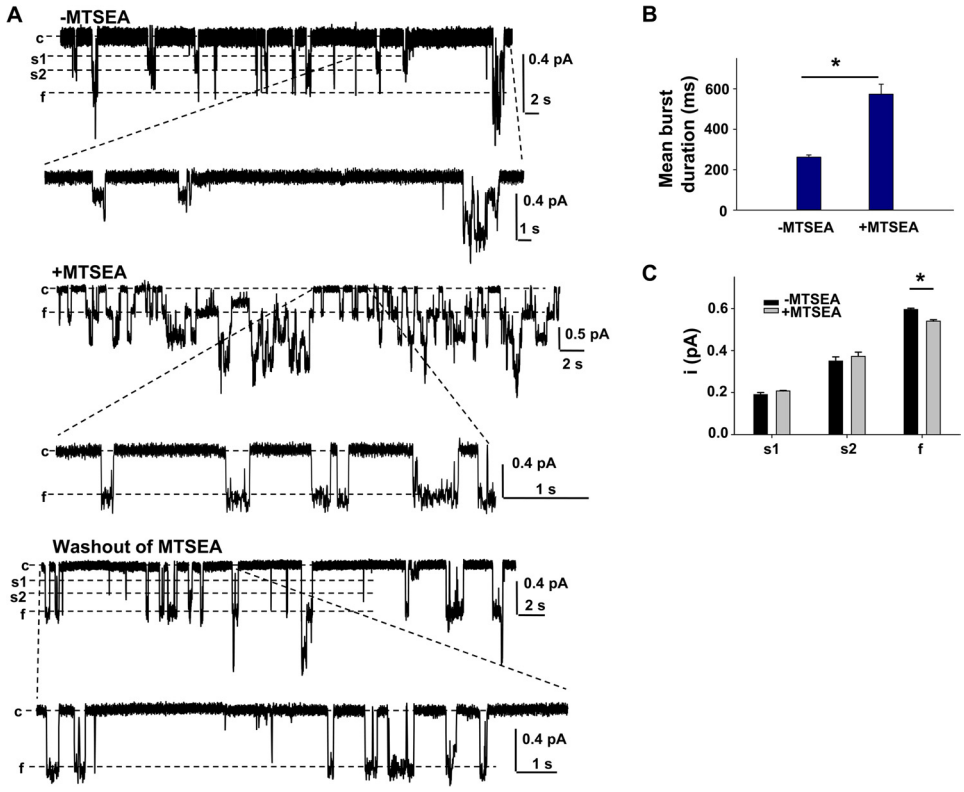

FIGURE 5. **Deposition of positive charge at R352C improved stability of the open state.** *A*, sample traces from R352C-CFTR recorded from one patch under control conditions (*top trace*, ATP + PKA) and in the presence of 100 μM $MTSEA^+$ (*middle trace*, ATP + PKA + $MTSEA^+$) and then after washout with a large volume of intracellular solution and the subsequent addition of ATP and PKA alone (*bottom trace*, ATP + PKA) in excised inside-out membrane patches. Sections of each of the three traces are also shown at expanded temporal resolution. All traces were recorded at $V_M = -100$ mV. *B*, comparison of mean burst duration of R352C in the absence of $MTSEA^+$ (ATP + PKA only) (*−MTSEA*) and in the presence of $MTSEA^+$ with ATP + PKA (*+MTSEA*). *C*, comparison of single channel amplitudes of the three open states of R352C-CFTR with or without 100 μM $MTSEA^+$. Single channel amplitudes of the s1 and s2 subconductance states remained unchanged, whereas the single channel amplitude of the f conductance state was significantly decreased after covalent modification with $MTSEA^+$ ($n = 5$). *Error bars*, S.E.

bridge function to stabilize channel behavior in R352C/D993C-CFTR in terms of stable openings to the f state (data not shown).

Before applying MTS-2-MTS to the R352C/D993C-CFTR double mutant, we first tested the effects of this bifunctional linker on WT-CFTR (Fig. 6*A*) and Cys-less V510A-CFTR (Fig. 6*B*). MTS-2-MTS did not change the single channel amplitude of either channel but decreased NP_o of WT-CFTR without changing NP_o of Cys-less V510A-CFTR. We then examined the effects of MTS-2-MTS on R352C-D993C-CFTR (on the WT-CFTR background); a representative experiment is shown in Fig. 7. In the presence of ATP and PKA, prior to the addition of MTS-2-MTS, R352C/D993C-CFTR exhibited low open probability, unstable openings to the f state, and occasional subconductance open states. After switching to solution containing ATP, PKA, and 100 μM MTS-2-MTS, the patch revealed two active channels, and both were latched nearly constitutively into the full open state. However, this was a fairly inefficient process, because in patches with multiple channels, not all channels would be locked open in each experiment. It seems likely that this reflects the fact that there are several possible consequences of exposing the double mutant to MTS-2-MTS, including covalent modification of R352C and D993C separately by two MTS-2-MTS molecules within each CFTR protein. In these cases, inspection of the traces allows identification of two separate pools of channels in a multichannel patch.

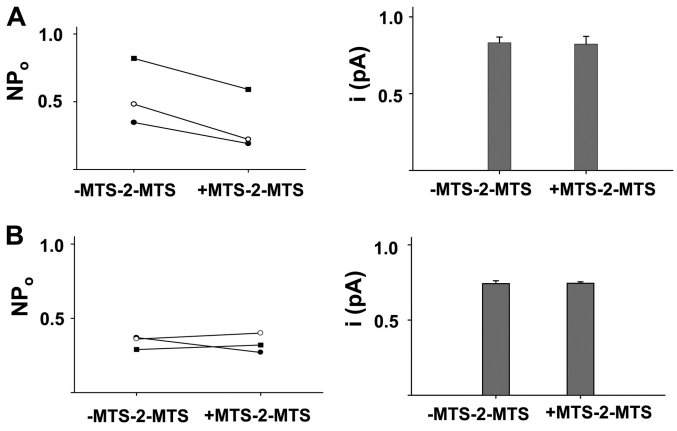

FIGURE 6. **Effects of 100 μM MTS-2-MTS on WT-CFTR (*A*) and Cys-less V510A-CFTR (*B*) at $V_M = -100$ mV.** *A*, MTS-2-MTS decreased NP_o but had no effect on single channel amplitude of WT-CFTR. *B*, the cross-linker had no effect on either NP_o or single channel amplitude of Cys-less V510A-CFTR. *Error bars*, S.E.

After washout with copious control solution free of ATP, PKA, and MTS-2-MTS, the channels remained in the full open state even after removal of ATP from the bath; subsequent exposure to 1 mM DTT caused channels to close. These results indicate that MTS-2-MTS was able to latch the channels open by formation of a covalent interaction that replicates the salt bridge formed between Arg^{352} and Asp^{993} in the wild type

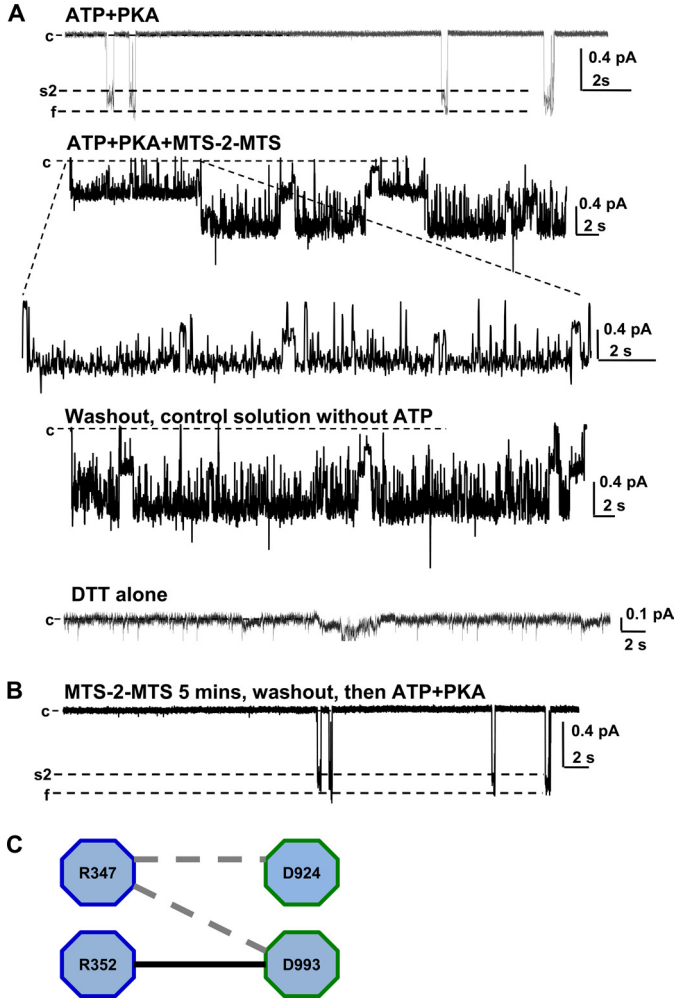

FIGURE 7. **MTS-2-MTS can latch open CFTR when applied to open channels.** *A*, effects of 100 μM MTS-2-MTS on R352C-D993C-CFTR. The data shown were recorded from one excised, inside-out patch under control conditions (*first trace*, ATP + PKA), in the presence of 100 μM MTS-2-MTS (*second trace*, ATP + PKA + MTS-2-MTS), in control conditions again (*fourth trace*), and in control conditions with DTT (*fifth trace*); the *third trace* presents part of the *second trace* at expanded temporal resolution, as indicated ($n = 4$). *B*, MTS-2-MTS failed to functionally modify R352C/D993C-CFTR when applied when the channel was in the closed state. The patch was incubated in control medium free of ATP and PKA, with 100 μM MTS-2-MTS, for >5 min, and then washed out with control solution, followed by exposure to ATP and PKA alone (representative of $n = 5$ patches with similar results). *C*, a schematic model of the salt bridges (*dashed gray line*, the triangular salt bridge contributing to the s2 state; *black line*, Arg^{352}-Asp^{993} salt bridge contributing to the f state). *Error bars*, S.E.

channel. Exposure to MTS-2-MTS when the channels were closed did not affect channel behavior upon subsequent exposure to ATP and PKA; the openings remained brief (Fig. 7*B*). These data strongly suggest that Arg^{352} and Asp^{993} approach each other closely as CFTR channels are opening and that the distance between them is about 4–6 Å when the channel is in the open state. In combination with the molecular dynamic simulation data from Dawson and Sansom (3), we conclude that Arg^{352} and Asp^{993} are at some distance from each other when the channel is in the closed state and move close to face each other as the channel opens.

To generate additional support for this conclusion, we applied the thermodynamic mutant cycle analysis approach to obtain quantitative evidence for the apparent interaction between Arg^{352} and Asp^{993} in the absence of cross-linker (22). Using this approach, if two amino acids do not interact with each other, the change in free energy upon mutation will be close to 0 kcal/mol; on the contrary, if two amino acids interact with each other, the change in free energy upon mutation will be above 1 kcal/mol or below −1 kcal/mol. The free energy change $\Delta\Delta G$ between WT-CFTR and R352C/D993C-CFTR was −1.508 kcal/mol, which suggests that R352C and D993C interact with each other when CFTR is in the open state (supplemental Fig. 5).

DISCUSSION

Multiple Open States of the CFTR Channel Result from Pore Conformational Changes—Subconductance states occur not only in CFTR but also in other channels and are attributed to several mechanisms (30–34). 1) Large conductance calcium-activated K^+ channels exhibit subconductance states, and flickers in the full open state result from channel pore conformational changes; 2) short lived subconductance states in Kv2.1 channels were found to be due to subunit interactions, and these processes are allosterically coupled; 3) subconductance states in L-type Ca^{2+} channels are produced from the different permeant ions, including Ca^{2+}, Ba^{2+}, and Li^+, that differ in binding affinity in the pore; 4) subconductance channel behavior in *Shaker* K channels, cyclic nucleotide-gated channels, and glutamate receptor channels has been associated with channel activation and inactivation (30–34).

It is known that WT-CFTR channels exhibit long stable openings and rare s1 and s2 states; also, there are frequent flickery closures within the long open bursts. We conclude that the subconductance states in CFTR probably also represent pore conformational change for the following reasons: 1) the CFTR channel pore forms from one polypeptide as a monomer and only bears one permeation pathway (12); 2) the s1 and s2 states occur as rare events in some point mutations, such as T338A/C- and K335A/C-CFTR, which do not appear to affect gross pore architecture, whereas they are frequent events in CFTR channels bearing salt bridge mutations, such as R352A- and R347A-CFTR, as discussed above; 3) mutations at sites involved in salt bridges (such as Arg^{347}, Arg^{352}, Asp^{924}, and Asp^{993}) result in much more frequent occupancy of subconductance states; 4) mutations at sites involved in salt bridges (such as Arg^{347} and Arg^{352}) lead to greatly altered sensitivity to pore blockers (7, 13); and 5) the subconductance behavior is not affected by different concentrations of Cl^- or by changes in membrane potential (12, 16). Here, we have provided evidence to suggest that gating in the CFTR channel requires coordinated and dynamic contributions from two different main domains of the protein: ATP-dependent gating at the cytoplasmic complex that includes the NBDs and the R domain and "pore gating" by conformational changes within the MSDs. It remains to be determined how the individual steps in ATP-dependent gating cooperate with conformational changes in the MSDs to control transitions between the multiple closed and open states that are exhibited by CFTR chloride channels.

Arg^{347}-Asp^{924}-Asp^{993} and Arg^{352}-Asp^{993} Cooperate to Maintain the CFTR Channel Pore in a Functional Architecture—In this paper, we have described a new interaction between Arg^{347}

and Asp^{993} as part of a complex triangular salt bridge, Arg^{347}-Asp^{924}-Asp^{993}, which is mainly involved in maintaining the s2 state (Fig. 7*C*). Arg^{352}-Asp^{993} (which plays a primary role in f state stability) and Arg^{347}-Asp^{924}-Asp^{993} cooperate to maintain the normal CFTR pore architecture when the channel is in the open state. The study is fundamentally based on changes in single channel behavior and changes in the s1, s2, and f states in different mutants. R347A-CFTR single channel traces clearly show that the channel first opens from the c to s1 state and then attempts to further open to the s2 and f state; we never saw the channel directly open from c to s2 or f in these mutants. Therefore, we believe that the process of CFTR channel pore opening probably proceeds from the closed state (c) → s1 → s2 or f. In WT-CFTR, the first stage of this process probably occurs at a rate of speed beyond the resolution of our recordings; thus, it is hard to see in WT channels but becomes clear in some mutants. Because the CFTR channel pore probably always first opens to the s1 state from the closed state, followed by transitions to the s2 or f state, it is reasonable to believe that both the Arg^{352}-Asp^{993} and Arg^{347}-Asp^{924}-Asp^{993} salt bridges are not formed when the channel is in the s1 state, but this is followed by the formation of the Arg^{347}-Asp^{924} and Arg^{347}-Asp^{993} salt bridges to maintain the s2 state, and then the Arg^{352}-Asp^{993} salt bridge forms to maintain f open state stability with possible breakage of Arg^{347}-Asp^{993}. These results suggest that Asp^{993} switches its interaction between Arg^{347} and Arg^{352} during the pore opening process. This flip-flopping salt bridge phenomenon also occurs in the bacterial channel OmpA, regarding the triangular salt bridge Arg^{138}-Glu^{52}-Lys^{82}, wherein switching of Glu^{52} between Arg^{138} and Lys^{82} is responsible for gating and defines the closed and open states of the channel (35, 36). Our data for the first time demonstrate that these two salt bridges in CFTR form sequentially rather than coincidentally and contribute unequally to maintaining CFTR pore structure and function but cooperate together to achieve the full goal of the stable open state. Taken together, the results suggest that small molecule drugs targeting intraprotein interaction sites in the MSDs may rescue the behavior of CFTR channels bearing mutations at these sites.

REFERENCES

1. Mornon, J. P., Lehn, P., and Callebaut, I. (2009) Molecular models of the open and closed states of the whole human CFTR protein. *Cell. Mol. Life Sci.* **66,** 3469–3486
2. Mornon, J. P., Lehn, P., and Callebaut, I. (2008) Atomic model of human cystic fibrosis transmembrane conductance regulator. Membrane-spanning domains and coupling interfaces. *Cell. Mol. Life Sci.* **65,** 2594–2612
3. Alexander, C., Ivetac, A., Liu, X., Norimatsu, Y., Serrano, J. R., Landstrom, A., Sansom, M., and Dawson, D. C. (2009) Cystic fibrosis transmembrane conductance regulator. Using differential reactivity toward channel-permeant and channel-impermeant thiol-reactive probes to test a molecular model for the pore. *Biochemistry* **48,** 10078–10088
4. Riordan, J. R., Rommens, J. M., Kerem, B., Alon, N., Rozmahel, R., Grzelczak, Z., Zielenski, J., Lok, S., Plavsic, N., and Chou, J. L. (1989) Identification of the cystic fibrosis gene. Cloning and characterization of complementary DNA. *Science* **245,** 1066–1073
5. Serohijos, A. W., Hegedus, T., Aleksandrov, A. A., He, L., Cui, L., Dokholyan, N. V., and Riordan, J. R. (2008) Phenylalanine-508 mediates a cytoplasmic-membrane domain contact in the CFTR 3D structure crucial to assembly and channel function. *Proc. Natl. Acad. Sci. U.S.A.* **105,** 3256–3261
6. Riordan, J. R., and Chang, X. B. (1992) CFTR, a channel with the structure of a transporter. *Biochim. Biophys. Acta* **1101,** 221–222
7. Cui, G., Song, B., Turki, H. W., and McCarty, N. A. (2012) Differential contribution of TM6 and TM12 to the pore of CFTR identified by three sulfonylurea-based blockers. *Pflugers Arch.* **463,** 405–418
8. Bai, Y., Li, M., and Hwang, T. C. (2011) Structural basis for the channel function of a degraded ABC transporter, CFTR (ABCC7). *J. Gen. Physiol.* **138,** 495–507
9. Bai, Y., Li, M., and Hwang, T. C. (2010) Dual roles of the sixth transmembrane segment of the CFTR chloride channel in gating and permeation. *J. Gen. Physiol.* **136,** 293–309
10. Wang, W., El Hiani, Y., and Linsdell, P. (2011) Alignment of transmembrane regions in the cystic fibrosis transmembrane conductance regulator chloride channel pore. *J. Gen. Physiol.* **138,** 165–178
11. Dawson, D. C., and Smith, S. S. (1997) Cystic fibrosis transmembrane conductance regulator. Permeant ions find the pore. *J. Gen. Physiol.* **110,** 337–339
12. Zhang, Z. R., Cui, G., Liu, X., Song, B., Dawson, D. C., and McCarty, N. A. (2005) Determination of the functional unit of the cystic fibrosis transmembrane conductance regulator chloride channel. One polypeptide forms one pore. *J. Biol. Chem.* **280,** 458–468
13. Cui, G., Zhang, Z. R., O'Brien, A. R., Song, B., and McCarty, N. A. (2008) Mutations at arginine 352 alter the pore architecture of CFTR. *J. Membr. Biol.* **222,** 91–106
14. Cotten, J. F., and Welsh, M. J. (1999) Cystic fibrosis-associated mutations at arginine 347 alter the pore architecture of CFTR. Evidence for disruption of a salt bridge. *J. Biol. Chem.* **274,** 5429–5435
15. Fuller, M. D., Zhang, Z. R., Cui, G., and McCarty, N. A. (2005) The block of CFTR by scorpion venom is state-dependent. *Biophys. J.* **89,** 3960–3975
16. Zhang, Z. R., Song, B., and McCarty, N. A. (2005) State-dependent chemical reactivity of an engineered cysteine reveals conformational changes in the outer vestibule of the cystic fibrosis transmembrane conductance regulator. *J. Biol. Chem.* **280,** 41997–42003
17. DeCaen, P. G., Yarov-Yarovoy, V., Sharp, E. M., Scheuer, T., and Catterall, W. A. (2009) Sequential formation of ion pairs during activation of a sodium channel voltage sensor. *Proc. Natl. Acad. Sci. U.S.A.* **106,** 22498–22503
18. DeCaen, P. G., Yarov-Yarovoy, V., Zhao, Y., Scheuer, T., and Catterall, W. A. (2008) Disulfide locking a sodium channel voltage sensor reveals ion pair formation during activation. *Proc. Natl. Acad. Sci. U.S.A.* **105,** 15142–15147
19. DeCaen, P. G., Yarov-Yarovoy, V., Scheuer, T., and Catterall, W. A. (2011) Gating charge interactions with the S1 segment during activation of a Na^+ channel voltage sensor. *Proc. Natl. Acad. Sci. U.S.A.* **108,** 18825–18830
20. Gnann, A., Riordan, J. R., and Wolf, D. H. (2004) Cystic fibrosis transmembrane conductance regulator degradation depends on the lectins Htm1p/EDEM and the Cdc48 protein complex in yeast. *Mol. Biol. Cell* **15,** 4125–4135
21. Fuller, M. D., Thompson, C. H., Zhang, Z. R., Freeman, C. S., Schay, E., Szakács, G., Bakos, E., Sarkadi, B., McMaster, D., French, R. J., Pohl, J., Kubanek, J., and McCarty, N. A. (2007) State-dependent inhibition of cystic fibrosis transmembrane conductance regulator chloride channels by a novel peptide toxin. *J. Biol. Chem.* **282,** 37545–37555
22. Lee, W. Y., and Sine, S. M. (2005) Principal pathway coupling agonist binding to channel gating in nicotinic receptors. *Nature* **438,** 243–247
23. Craven, K. B., Olivier, N. B., and Zagotta, W. N. (2008) C-terminal movement during gating in cyclic nucleotide-modulated channels. *J. Biol. Chem.* **283,** 14728–14738
24. Craven, K. B., and Zagotta, W. N. (2004) Salt bridges and gating in the COOH-terminal region of HCN2 and CNGA1 channels. *J. Gen. Physiol.* **124,** 663–677
25. Kunzelmann, K., Kiser, G. L., Schreiber, R., and Riordan, J. R. (1997) Inhibition of epithelial Na^+ currents by intracellular domains of the cystic fibrosis transmembrane conductance regulator. *FEBS Lett.* **400,** 341–344
26. Drumm, M. L., Wilkinson, D. J., Smit, L. S., Worrell, R. T., Strong, T. V., Frizzell, R. A., Dawson, D. C., and Collins, F. S. (1991) Chloride conductance expressed by ΔF508 and other mutant CFTRs in *Xenopus* oocytes. *Science* **254,** 1797–1799

27. Mense, M., Vergani, P., White, D. M., Altberg, G., Nairn, A. C., and Gadsby, D. C. (2006) *In vivo* phosphorylation of CFTR promotes formation of a nucleotide-binding domain heterodimer. *EMBO J.* **25,** 4728–4739
28. Holstead, R. G., Li, M. S., and Linsdell, P. (2011) Functional differences in pore properties between wild-type and cysteine-less forms of the CFTR chloride channel. *J. Membr. Biol.* **243,** 15–23
29. Aubin, C. N., and Linsdell, P. (2006) Positive charges at the intracellular mouth of the pore regulate anion conduction in the CFTR chloride channel. *J. Gen. Physiol.* **128,** 535–545
30. Marchais, D., and Marty, A. (1979) Interaction of permeant ions with channels activated by acetylcholine in *Aplysia* neurones. *J. Physiol.* **297,** 9–45
31. Swenson, R. P., Jr., and Armstrong, C. M. (1981) K^+ channels close more slowly in the presence of external K^+ and Rb^+. *Nature* **291,** 427–429
32. Pusch, M., Steinmeyer, K., Koch, M. C., and Jentsch, T. J. (1995) Mutations in dominant human myotonia congenita drastically alter the voltage dependence of the CIC-1 chloride channel. *Neuron* **15,** 1455–1463
33. Schneggenburger, R., and Ascher, P. (1997) Coupling of permeation and gating in an NMDA-channel pore mutant. *Neuron* **18,** 167–177
34. Yang, J., Yu, M., Jan, Y. N., and Jan, L. Y. (1997) Stabilization of ion selectivity filter by pore loop ion pairs in an inwardly rectifying potassium channel. *Proc. Natl. Acad. Sci. U.S.A.* **94,** 1568–1572
35. Hong, H., Szabo, G., and Tamm, L. K. (2006) Electrostatic couplings in OmpA ion-channel gating suggest a mechanism for pore opening. *Nat. Chem. Biol.* **2,** 627–635
36. Moroni, A., and Thiel, G. (2006) Flip-flopping salt bridges gate an ion channel. *Nat. Chem. Biol.* **2,** 572–573